free energy of desolvation for the larger neo-pentyl system relative to the methyl chloride system (*33*). Initial work indicates that the difference in free energy of solvation between the methyl chloride and neopentyl chloride reactions in water is about 4 kcal/mol, suggesting that the observed barrier in solution would be that much greater than the intrinsic barrier.

In summary, differential solvation of the transition states accounts for a significant part of the barrier differences in solution and explains the difference seen between gas-phase and solution-phase experimental results for the S_N2 reaction.

References and Notes

1. A. W. Hofmann, *Ber. Dtsch. Chem. Ges.* **5**, 704 (1872).
2. _____ , *Ber. Dtsch. Chem. Ges.* **8**, 61 (1875).
3. C. K. Ingold, *Structure and Mechanism in Organic Chemistry* (Cornell Univ. Press, Ithaca, NY, ed. 2, 1969).
4. T. H. Lowry, K. S. Richardson, *Mechanism and Theory in Organic Chemistry* (HarperCollins, New York, 1987).
5. M. S. Newman, Ed., *Steric Effects in Organic Chemistry* (Wiley, New York, 1956).
6. A. G. Evans, M. Polanyi, *Nature* **149**, 608 (1942).
7. P. B. D. De La Mare, L. Fowden, E. D. Hughes, C. K. Ingold, J. D. H. Mackie, *J. Chem. Soc.*, 3200 (1955).
8. The calculated steric energy remained high in the case of neopentyl chloride. Ingold acknowledged that the classical treatment could not consider all important interactions in a timely manner.
9. A. Streitwieser, *Solvolytic Displacement Reactions* (McGraw-Hill, New York, 1962).
10. W. N. Olmstead, J. I. Brauman, *J. Am. Chem. Soc.* **99**, 4219 (1977).
11. M. L. Chabinyc, S. L. Craig, C. K. Regan, J. I. Brauman, *Science* **279**, 1882 (1998).
12. R. A. Marcus, *J. Phys. Chem. A* **101**, 4072 (1997).
13. M. J. Pellerite, J. I. Brauman, *J. Am. Chem. Soc.* **105**, 2672 (1983).
14. G. Caldwell, T. F. Magnera, P. Kebarle, *J. Am. Chem. Soc.* **106**, 959 (1984).
15. S. E. Barlow, J. M. V. Doren, V. M. Bierbaum, *J. Am. Chem. Soc.* **110**, 7240 (1988).
16. J. M. Riveros, S. M. Jose, K. Takashima, *Adv. Phys. Org. Chem.* **21**, 197 (1985).
17. C. H. DePuy, S. Gronert, A. Mullin, V. M. Bierbaum, *J. Am. Chem. Soc.* **112**, 8650 (1990).
18. S. Gronert, *Chem. Rev.* **101**, 329 (2001).
19. B. D. Wladkowski, K. F. Lim, W. D. Allen, J. I. Brauman, *J. Am. Chem. Soc.* **114**, 9136 (1992).
20. W. L. Hase, *Science* **266**, 998 (1994).
21. A. A. Viggiano *et al.*, *J. Am. Chem. Soc.* **116**, 2213 (1994).
22. S. L. Craig, J. I. Brauman, *Science* **276**, 1536 (1997).
23. M. Zhong, J. I. Brauman, *J. Am. Chem. Soc.* **118**, 636 (1996).
24. **1** was obtained from Aldrich, and **2** was synthesized according to literature procedures (*34, 35*). Both compounds were purified by low-pressure distillation and preparative gas chromatography before use to ensure that the slow reactions would not be affected by impurities. Chloride ion was generated by electron impact ionization on the chloronitrile under study.
25. J. W. Larson, T. B. McMahon, *Can. J. Chem.* **62**, 675 (1984).
26. _____ , *J. Am. Chem. Soc.* **106**, 517 (1984).
27. _____ , *J. Am. Chem. Soc.* **107**, 766 (1985).
28. We used ΔE_{diff} as a measure of the steric effect. ΔE_{diff} actually contains the differential effect of polarizability between separated reactants and transition states in addition to the energy of the steric effect. Another choice for the measure of the steric effect (ΔE^*), the S_N2 barrier height as measured from the bottom of the well, controls for differences in polarizability. That difference is small in the comparison between the complexes of chloride ion with **1** and **2**.
29. R. G. Gilbert, S. C. Smith, *Theory of Unimolecular and Recombination Reactions* (Blackwell Scientific, Oxford, 1990).
30. J. Chandrasekhar, S. F. Smith, W. L. Jorgensen, *J. Am. Chem. Soc.* **106**, 3049 (1984).
31. _____ , *J. Am. Chem. Soc.* **107**, 154 (1985).
32. J. Chandrasekhar, W. L. Jorgensen, *J. Am. Chem. Soc.* **107**, 2974 (1985).
33. W. L. Jorgensen, *BOSS, Version 3.8* (Yale University, New Haven, CT, 1997).
34. J. W. Davis, *J. Org. Chem.* **43**, 3980 (1978).
35. R. M. Carman, I. M. Shaw, *Aust. J. Chem.* **29**, 133 (1976).
36. Supported by the NSF. Funded by fellowships from the General Electric Foundation (C.K.R.); the NSF, ACS Division of Organic Chemistry, DuPont Merck Pharmaceutical Fellowship; and the Stanford University, John Stauffer Memorial Fellowship (S.L.C.). We are grateful to W. L. Jorgensen and his research group for helpful discussions.

Liquid-State NMR and Scalar Couplings in Microtesla Magnetic Fields

Robert McDermott,[1,3]* Andreas H. Trabesinger,[2,3] Michael Mück,[4] Erwin L. Hahn,[1] Alexander Pines,[2,3] John Clarke[1,3]
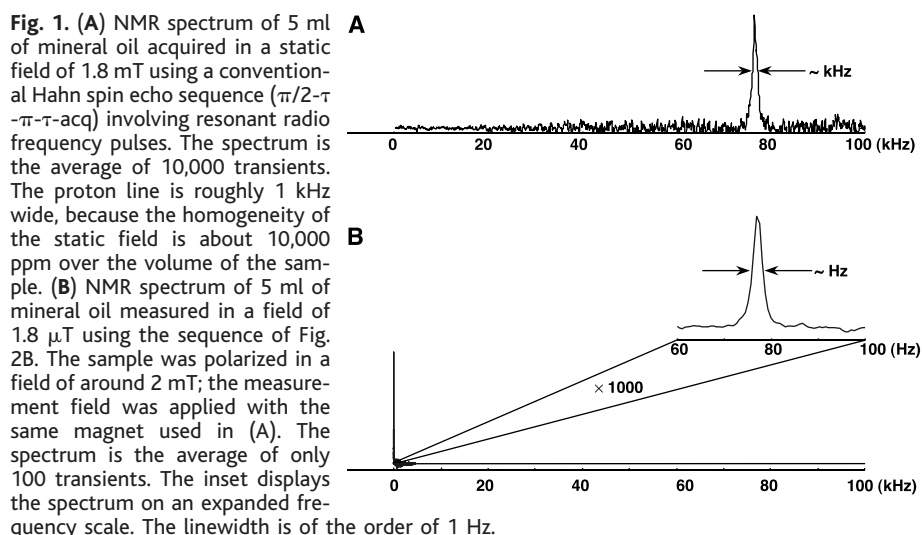
We obtained nuclear magnetic resonance (NMR) spectra of liquids in fields of a few microtesla, using prepolarization in fields of a few millitesla and detection with a dc superconducting quantum interference device (SQUID). Because the sensitivity of the SQUID is frequency independent, we enhanced both signal-to-noise ratio and spectral resolution by detecting the NMR signal in extremely low magnetic fields, where the NMR lines become very narrow even for grossly inhomogeneous measurement fields. In the absence of chemical shifts, proton-phosphorous scalar (J) couplings have been detected, indicating the presence of specific covalent bonds. This observation opens the possibility for "pure J spectroscopy" as a diagnostic tool for the detection of molecules in low magnetic fields.

In high-field, liquid-state nuclear magnetic resonance (NMR) spectroscopy, chemical shifts and electron-mediated scalar spin-spin (J) couplings yield diagnostic information about chemical bonding and molecular structure (*1*). The information content of the spectrum is often limited by spectral resolution, which is determined by the width of the NMR lines. To attain the resolution necessary to distinguish different resonance lines, very high field homogeneity (a few parts per billion) is required. In modern commercial NMR spectrometers, homogeneity is achieved by supplementing the large magnet with sophisticated and meticulously tuned shim coils.

[1]Department of Physics and [2]Department of Chemistry, University of California, Berkeley, CA 94720, USA. [3]Materials Sciences Division, Lawrence Berkeley National Laboratory, Berkeley, CA 94720, USA. [4]Institute of Applied Physics, University of Giessen, Giessen D-35392 Germany.

*To whom correspondence should be addressed. E-mail: rmcderm@socrates.berkeley.edu

Fig. 1. (A) NMR spectrum of 5 ml of mineral oil acquired in a static field of 1.8 mT using a conventional Hahn spin echo sequence ($\pi/2$-τ-π-τ-acq) involving resonant radio frequency pulses. The spectrum is the average of 10,000 transients. The proton line is roughly 1 kHz wide, because the homogeneity of the static field is about 10,000 ppm over the volume of the sample. **(B)** NMR spectrum of 5 ml of mineral oil measured in a field of 1.8 μT using the sequence of Fig. 2B. The sample was polarized in a field of around 2 mT; the measurement field was applied with the same magnet used in (A). The spectrum is the average of only 100 transients. The inset displays the spectrum on an expanded frequency scale. The linewidth is of the order of 1 Hz.

However, for many applications of NMR, it may be impractical or unfavorable to place the object or subject of study in the bore of a high-field magnet. Moreover, even when high-field magnets are accessible, heterogeneous samples, such as organisms studied by in vivo spectroscopy or porous rocks encountered in oil well logging, are subject to variations in magnetic susceptibility over the sample volume; these variations produce spurious gradients that broaden the resonance lines.

Techniques have been developed which yield information about spin relaxation and diffusion processes in samples measured in extremely inhomogeneous fields, and their utility for the nondestructive characterization of materials has been demonstrated (2). Furthermore, a recently reported "ex situ" NMR technique enables the recovery of chemical shift information in the presence of field inhomogeneity (3). However, these methods still require high magnetic fields and do not mitigate the effects of magnetic susceptibility broadening.

An appealing alternative approach to conventional high resolution NMR is the possibility of spectroscopy in extremely low magnetic fields. In the past, studies in the Earth's field range (approximately 50 μT) were motivated by the high cost and complexity of the high field equipment (4–6). Little attention has been paid to the fact that, for a fixed relative homogeneity, the NMR linewidth scales linearly with the strength of the magnetic field. Therefore, by reducing the strength of the measurement field, it is possible to achieve very narrow NMR lines and associated high signal-to-noise (S/N) ratio and spectral resolution. Chemical shifts are unresolved at such low fields, but scalar couplings, which are field-independent, are preserved. These scalar coupling strengths act as signatures of specific covalent bonds (7–10).

The obvious obstacles to low-field experiments are that the thermal polarization of the nuclear spins scales with magnetic field, and that the conventional NMR detector, which is sensitive to the rate of change of magnetic flux, produces a voltage that scales with Larmor frequency, and hence with magnetic field. The loss in polarization can be circumvented by one of several techniques which create enhanced, non-equilibrium nuclear spin polarization, such as dynamic nuclear polarization (DNP) (11, 12), optical pumping (13), or prepolarization (14). The consequence of Faraday's Law can be avoided by detecting with a dc superconducting quantum interference device (SQUID) (15), which is sensitive to magnetic flux, rather than the rate of change of flux. When operated with an untuned (superconducting) input circuit, the SQUID detects broadband at arbitrarily low frequencies without a loss in sensitivity.

SQUIDs have been used successfully since the 1980s to detect NMR signals (16). The majority of SQUID NMR measurements have been performed on samples in the solid state at liquid helium temperatures. However, more recently, Seton et al. (17) used SQUIDs to image room temperature samples in fields of several millitesla. Kumar et al. (18) demonstrated spectra from animal tissue at room temperature, and Schlenga et al. (19) used a SQUID magnetometer fabricated from the high transition temperature superconductor $YBa_2Cu_3O_{7-x}$ to image thermally polarized proton samples at room temperature in comparable fields.

In our experiments, we use an untuned low transition temperature (low T_c) SQUID to measure NMR signals from liquid samples in considerably lower fields—a few microtesla—where the proton Larmor frequency is of the order of 100 Hz. At these fields, a homogeneity of 10,000 ppm is sufficient to give a spectral resolution of the order of 1 Hz, comparable to the resolution achieved in state-of-the-art high field spectrometers.

Figure 1 illustrates the S/N ratio enhancement associated with measurement in microtesla magnetic fields. In a static field of 1.8 mT, the proton resonance from a sample of mineral oil is broadened to about 1 kHz (Fig. 1A). Thousands of averages were required before the line could be clearly resolved. By contrast, the proton resonance from mineral oil measured in the same experimental setup at a field of 1.8 μT has a linewidth of the order of 1 Hz (Fig. 1B). As the SQUID magnetometer was untuned, the NMR signal strength was independent of Larmor frequency for a given sample magnetization, that is, the area under the NMR line was conserved. For a given magnetic field inhomogeneity, the width of the NMR line scales linearly with the measurement field, and so the peak height and the S/N ratio are enhanced as the measurement field is reduced. When the proton resonance was lowered from 77 kHz to 77 Hz, the NMR line-

Fig. 2. (A) Schematic of SQUID spectrometer for microtesla field NMR. The detector used was a Nb-AlOx-Nb dc SQUID. The dc SQUID consists of a superconducting loop interrupted by two Josephson junctions (15). When biased with a current I_b slightly above the critical current of the junctions, the SQUID acts as a flux-to-voltage transducer. To enhance its sensitivity to magnetic fields, the SQUID is often operated with a superconducting flux transformer consisting of a pickup coil tightly coupled to the sample and an input coil tightly coupled to the SQUID loop. The flux transformer operates on the principle of flux conservation in a superconducting loop, which involves no frequency dependence. Thus, the SQUID magnetometer can detect broadband at arbitrarily low frequencies with no loss in sensitivity. In these experiments, the input coil (with inductance L_i) of the transformer was integrated onto the SQUID chip; the niobium wire pickup coil (with inductance L_p) was wound in a gradiometric fashion around the tail section of a cryogenic insert, made of Pyrex, which was surrounded by liquid helium. A Pyrex cell containing the liquid sample was lowered into the tail of the insert; a resistive heater maintained the sample temperature at around 300 K. A single-layer solenoid of copper wire wound directly on the sample cell produced the polarizing field. A set of coils located in the helium bath provided the measurement field. The belly of the helium dewar was lined with a superconducting Pb sheet, and the dewar was surrounded by a single-layer mu-metal shield to attenuate both the static magnetic field of the Earth and external magnetic fluctuations. The SQUID was operated in a flux-locked loop with modulation at 2 MHz, and the signal from the SQUID was amplified, integrated, and fed back to the SQUID as a magnetic flux. The voltage across the feedback resistor R_f was thus proportional to applied flux. In this way, the SQUID acted as a null detector of magnetic flux. **(B)** Pulse sequence for microtesla field NMR. The sample was polarized in a field B_p of about 1 mT for a time that is long compared to the spin-lattice relaxation time of the sample (typically several seconds). In addition, a measurement field B_m of a few microtesla was applied in an orthogonal direction. When the polarizing field was removed nonadiabatically, the spins precessed in the measurement field. As the spins precessed, they lost phase coherence due to the poor homogeneity of the measurement field. At a time τ after removing the polarization field, the direction of the measurement field was abruptly reversed, causing the spins to reverse the sense of their precession. During the interval from τ to 2τ, phase coherence was restored, and at a time 2τ, the echo amplitude was a maximum. This field inversion spin echo is to be contrasted with the conventional Hahn spin echo (22), in which the phase of the spins is inverted by means of radio frequency pulses, but the sense of precession is preserved.
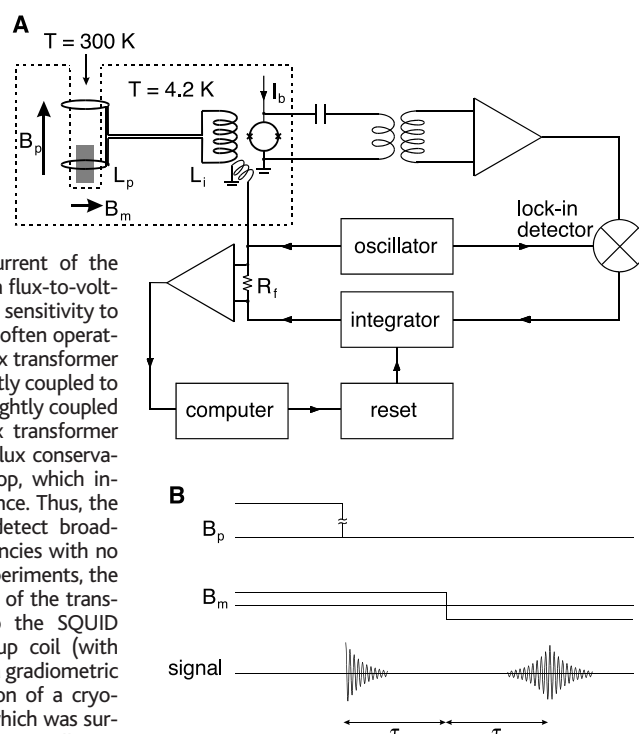
width was compressed by a factor of 1000, and the peak height grew by the same factor. In measurement fields of order 1 μT, we achieved a S/N ratio of a few tens without signal averaging from samples with a volume of a few milliliters and a polarization of order 10^{-8} (20).

Figure 2A shows a schematic of the apparatus; Fig. 2B outlines the experimental approach. A polarizing field of about 1 mT was applied to the sample. The much lower measurement field was applied in a direction orthogonal to the polarizing field. When the polarizing field was reduced nonadiabatically to zero, the sample magnetization precessed in the measurement field. Magnetic transients associated with the rapid turnoff of the polarizing field saturated the detector, giving a deadtime on the order of tens of milliseconds and necessitating the use of a spin echo to refocus the sample magnetization. The echo was formed by reversing the direction of the measurement field, and therefore the sense of precession of the nuclear spins.

Operation of the SQUID magnetometer in an untuned mode enables detection over a broad band. Moreover, as the sequence of Fig. 2B involves switched static fields rather than resonant spin manipulation, excitation occurs over a broad band. Our experimental scheme is therefore ideally suited to studies of systems containing nuclear spins with different magnetogyric ratios, that resonate at different frequencies. Figure 3 demonstrates simultaneous SQUID detection of ^{1}H and ^{31}P resonances.

The enhanced spectral resolution achieved by measuring in microtesla fields can be exploited to detect scalar couplings in heteronuclear spin systems. Figure 4 demonstrates that the presence or formation of a chemical bond can be observed through the detection of J couplings. The proton NMR spectrum of a mixture of phosphoric acid and methanol at 4.8 μT (Fig. 4A) consists of a sharp singlet, but for the ester trimethyl phosphate, which can be formed from the reaction of phosphoric acid and methanol, the line splits into a doublet, characteristic of J coupling between the proton spins and the ^{31}P nucleus, with a coupling strength $J_3[P,H] = 10.4 \pm 0.6$ Hz (Fig. 4B). In general, because electron-mediated scalar couplings between nuclear spins act as signatures of specific covalent bonds, the techniques outlined here could form the basis of a simple low-field NMR "bond detector," insensitive to chemical shifts, but yielding accurate information about heteronuclear couplings. Such a detector could be applied to the study of analytes, chemical reactions, and molecular conformations. For example, the dispersion of J-values for sp^3 ^{1}H-^{13}C bonds is approximately 10 times greater than the NMR linewidths achieved in our experiments. If the values of the J-coupling are known, then pure J-spectra could allow one to assign a number of molecular groups. Considering the highly developed techniques for isotopic labeling in biomolecular NMR, the use of such a method for following a "spy nucleus" through bond formation is an appealing possibility.

Finally, we note that the technique of bandwidth-narrowing through measurement in microtesla fields can also be applied to magnetic resonance imaging (MRI). In an MRI experiment, the ultimate spatial resolution is determined by the width of the NMR line in the absence of applied magnetic field gradients. For an MRI experiment performed in low field with linewidths approaching the lifetime limit, relatively high spatial resolution should be achievable with modest magnetic field gradients. As a result the NMR signal is dispersed over only a narrow band, resulting in a high S/N ratio, and thus a short acquisition time. Furthermore, distortions due to spurious gradients generated as a result of spatial variations in magnetic susceptibility should be minimized in low field (21).

References and Notes

1. R. R. Ernst, G. Bodenhausen, A. Wokaun, *Principles of Nuclear Magnetic Resonance in One and Two Dimensions* (Oxford Univ. Press, Oxford, 1987).
2. B. Blumich *et al.*, *Magn. Reson. Imaging* **16**, 479 (1998).
3. C. A. Meriles, D. Sakellariou, H. Heise, A. J. Moule, A. Pines, *Science* **293**, 82 (2001).
4. G. J. Bene, *Phys. Rep.* **58**, 213 (1980).
5. D. D. Thompson, R. J. S. Brown, *J. Chem. Phys.* **35**, 1894 (1961).
6. _____, *J. Chem. Phys.* **36**, 2812 (1962).
7. Field-independent interactions have been studied by zero-field NMR, mainly in solid samples. These studies rely either on strong interactions, as in the case of pure nuclear quadrupole resonance (NQR) (8), or on coherent evolution in zero field combined with polarization and detection in high field (field cycling) (9). The latter method was also used to obtain zero-field spectra of J-coupled liquids (10).
8. A. N. Garroway *et al.*, *IEEE Trans. Geosci. Remote Sens.* **39**, 1108 (2001).
9. D. B. Zax, A. Bielecki, K. W. Zilm, A. Pines, D. P. Weitekamp, *J. Chem. Phys.* **83**, 4877 (1985).
10. D. B. Zax, A. Bielecki, K. W. Zilm, A. Pines, *Chem. Phys. Lett.* **106**, 550 (1984).
11. A. Abragam, M. Goldman, *Nuclear Magnetism: Order and Disorder* (Clarendon, Oxford, 1982).
12. C. P. Slichter, *Principles of Nuclear Magnetic Resonance* (Springer Verlag, New York, ed. 3, 1990).
13. W. Happer *et al.*, *Phys. Rev. A* **29**, 3092 (1984).
14. M. Packard, R. Varian, *Phys. Rev.* **93**, 941 (1954).
15. J. Clarke, in *SQUID Sensors: Fundamentals, Fabrication and Applications*, H. Weinstock, Ed. (Kluwer Academic, Dordrecht, Netherlands, 1996), pp. 1–62.
16. Ya. S. Greenberg, *Rev. Mod. Phys.* **70**, 175 (1998).
17. H. C. Seton, J. M. S. Hutchison, D. M. Bussell, *Meas. Sci. Technol.* **8**, 198 (1997).
18. S. Kumar, B. D. Thorson, W. F. Avrin, *J. Magn. Reson. B* **107**, 252 (1995).
19. K. Schlenga *et al.*, *Appl. Phys. Lett.* **75**, 3695 (1999).
20. By way of comparison, a 700 MHz NMR spectrometer provides S/N ratios of order 10^4 to 10^5 from spins with thermal polarizations of approximately 6×10^{-5}.
21. C. H. Tseng *et al.*, *Phys. Rev. Lett.* **81**, 3785 (1998).
22. E. L. Hahn, *Phys. Rev.* **80**, 580 (1950).
23. Supported by the Director, Office of Science, Office of Basic Energy Sciences, Materials Sciences Division of the U.S. Department of Energy under contract DE-AC03-76SF00098. A.H.T. acknowledges the Swiss National Science Foundation for support through a postdoctoral fellowship.

Fig. 3. NMR spectrum of 5 ml of 85% phosphoric acid (H_3PO_4) measured in a field of 2.6 μT. The spectrum is the average of 1000 transients. The magnetogyric ratios of the spin-1/2 nuclei ^{1}H and ^{31}P differ by a factor of 2.5. The ^{1}H resonance appears at 110 Hz, while the ^{31}P resonance is clearly resolved at 44 Hz. The relative intensity of the two lines is determined by the different spin densities of the two nuclear species, as well as by the difference in thermal magnetizations brought about as a result of the difference in magnetogyric ratios.
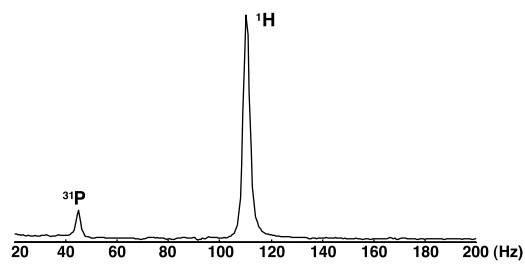

Fig. 4. (**A**) NMR spectrum of 5 ml of 3 parts methanol, 1 part phosphoric acid (85% in water) measured in a field of 4.8 μT. The spectrum is the average of 100 transients. Rapid spin exchange with the protons in water obscures the proton-phosphorous scalar coupling in phosphoric acid, and the proton spectrum consists of a sharp singlet. (**B**) NMR spectrum of 3 ml of neat trimethyl phosphate (Sigma-Aldrich) measured in a field of 4.8 μT. The spectrum is the average of 100 transients. Electron-mediated scalar coupling of the nine equivalent protons to the ^{31}P nucleus splits the proton resonance into a doublet, with a splitting that is determined by the coupling strength J. For this particular coupling via three covalent bonds, $J_3[P,H] = 10.4 \pm 0.6$ Hz. Scalar coupling to the nine protons splits the ^{31}P resonance into a decuplet; those lines are below the noise level. The reduction in S/N ratio is due to the lower sample volume and filling factor.